Lab on a Chip

PRESCIENT: Platform for the Rapid Evaluation of Antibody Success using Integrated Microfluidics Enabled Technology

Journal:	*Lab on a Chip*
Manuscript ID	LC-ART-11-2019-001165.R1
Article Type:	Paper
Date Submitted by the Author:	31-Jan-2020
Complete List of Authors:	Wippold, Jose; Texas A&M University System, Biomedical Engineering; Wang, Han; Texas A&M University, Dept. Electrical and Computer Engineering Tingling, Joseph; Texas A&M University System, Department of Microbial Pathogenesis and Immunology Leibowitz, Julian; Texas A&M University System, Department of Microbial Pathogenesis and Immunology de Figueiredo, Paul; Texas A&M University, Department of Plant Pathology and Microbiology Han, Arum; Texas AandM University, ECE Department

PRESCIENT: Platform for the Rapid Evaluation of Antibody Success using Integrated Microfluidics Enabled Technology

Jose A. Wippold[a], Han Wang[b,c], Joseph Tingling[d], Julian Leibowitz[d], Paul de Figueiredo[d,e,f,1], Arum Han[a,b,1].

[a]Department of Biomedical Engineering, Texas A&M University, College Station, TX 77843, USA; [b]Department of Biomedical Engineering, School of Medicine, Tsinghua University, Beijing, CHINA. [c]Department of Electrical and Computer Engineering, Texas A&M University, College Station, TX 77843, USA; [d]Department of Microbial Pathogenesis and Immunology, Texas A&M Health Science Center, Bryan, TX 77807, USA; [e]Norman Borlaug Center, Texas A&M University, College Station, TX 77843, USA; [f]Department of Veterinary Medicine, Texas A&M University, College Station, TX 77843

[1]To whom correspondence may be addressed. Email: arum.han@ece.tamu.edu or pjdefiguiredo@tamu.edu

Abstract

Identifying antibodies (Abs) that neutralize infectious agents is the first step for developing therapeutics, vaccines, and diagnostic tools for those infectious agents. However, current approaches for identifying neutralizing Abs (nAbs) typically rely on dilution-based assays that are costly, inefficient, and only survey a small subset of the entire repertoire. There are also intrinsic biases in many steps of conventional nAb identification processes. More importantly, conventional assays rely on simply Ab-antigen binding assays, which may not result in identifying the most potent nAbs, as the strongest binder may not be the most potent nAb. Droplet microfluidic systems have the capability to overcome such limitations by conducting complex multi-step assays with high reliability, resolution, and throughput in a pico-liter volume water-in-oil emulsion droplet format. Here, we describe the development of PRESCIENT (Platform for the Rapid Evaluation of antibody SucCess using Integrated microfluidics ENabled Technology), a droplet microfluidic system that can enable high-throughput single-cell resolution identification of nAb repertoires elicited in response to a viral infection. We demonstrated PRESCIENT's ability to identify Abs that neutralize a model viral agent, *Murine coronavirus* (Murine Hepatitis Virus), which causes high mortality rates in experimentally infected mice. In-droplet infection of host cells by the virus was first demonstrated, followed by demonstration of in-droplet neutralization by nAbs produced from a single Ab-producing hybridoma cell. Finally, fluorescent intensity analyses of two populations of hybridoma cell lines, (nAb-producing and non-nAb-producing hybridoma cell lines) successfully discriminated between the two populations. The presented strategy and platform have the potential to identify and investigate neutralizing activities against a broad range of potential

infectious agents for which nAbs have yet to be discovered, significantly advancing the nAb identification process, as well as reinvigorating the field of Ab discovery, characterization, and development.

Introduction

Some of the most promising strategies to combat virulent infectious diseases include the use of pathogen-specific neutralizing antibodies (nAbs), which form a basis towards development of Ab therapeutics or vaccines that elicit nAbs (1, 2). Standard approaches to nAb discovery typically start by either generating hybridomas from primary B cells or utilizing display systems such as phage or bacteria, followed by Ab-antigen binding assays (3, 4). However, there are several fundamental limitations inherent in these approaches. First, standard approaches have intrinsic biases at multiple stages during Ab generation and evaluation processes, primarily due to the necessity of generating immortalized Ab-secreting hybridoma cells (5). These cells can be used as a consistent and dependable source of Ab supply (6). However, hybridoma generation techniques are inefficient and cannot reliably transform the entire sample population, thus resulting in significant losses in the diversity of the population, and as a consequence, leading to high levels of biases in the samples being screened (7, 8). Second, the entire repertoire of Abs produced by an individual's B cell population is approximately 10 billion (9). Thus, even for the relatively high throughput limiting dilution approaches conventionally used for isolating and characterizing the properties of Abs produced by individual B cells, it becomes too costly and time-consuming to perform such analyses on large populations (10, 11). Third, and perhaps the biggest limitation of current approaches, is their dependency on a simple antigen-Ab binding assay, which may not result in identifying the most potent nAbs (2, 4, 7, 12, 13). While widely utilized, these tests alone cannot determine if Ab binding to antigen actually prevents infection of a host cell. Moreover, the strongest binder may not be the most potent neutralizer. Together, these confounding features result in the need for further testing in the form of functional neutralization screens that can determine the true activity of the Ab candidates (13). Conducting functional neutralization screens also requires multiple assay steps. Therefore, performing such a complex assay for a large number of Ab-producing B cells or display library is extremely time-consuming, costly, and labor-intensive, which is why most nAb discovery campaigns rely on Ab-antigen binding assays rather than direct assays that test the Ab functionality (8, 14, 15). Taken together, these limitations dramatically constrain the diversity of Ab repertoires that can be tested,

reducing the number of potentially useful nAbs that can be discovered, often leading to unsuccessful outcomes (15).

Droplet microfluidics platforms, where water-in-oil emulsion droplets function as individual pico-liter-scale bioreactors and where such cell-encapsulated droplets can be generated and undergo various assays at extremely high throughput, have revolutionized the field of high-throughput single-cell assays (16-23). Using such platforms, hybridoma screening for Abs that bound to known targets has been demonstrated in a droplet microfluidics format (24, 25); however this analysis was neither performed in the context of viral infection, nor employed to identify neutralizing activities. More recently, a droplet microfluidic system was utilized in binding assays that map epitopes that recognize broadly neutralizing Abs (26). However, there is still no microfluidic system where neutralization of viral infection of host cells can be directly measured and detected. To address these limitations, we developed the PRESCIENT (Platform for the Rapid Evaluation of antibody SucCess using Integrated microfluidics ENabled Technology) system, a high-throughput droplet-microfluidics-based lab-on-a-chip system that has the potential to directly identify nAbs through an in-droplet functional neutralization assay. PRESCIENT directly measures whether host cell infection by a virus is prevented, paving the way for the identification of nAbs that can then be advanced towards therapeutic nAb development and/or vaccine development. The developed system was utilized to successfully conduct in-droplet infection of host cells by Murine Hepatitis Virus (MHV), neutralization of such infection by nAbs produced from a single hybridoma cell encapsulated in a droplet, and a mock screening assay utilizing two different hybridoma population, one that produces nAbs and a another that produces non-neutralizing Abs, respectively.

Results

Overview of the PRESCIENT System

The PRESCIENT system (Fig. 1) is designed to sequentially perform the following basic functions: generation of large numbers of water-in-oil emulsion droplets encapsulating Ab-producing cells, each serving as independent pico-liter scale bioreactors; incubation of the cell-encapsulated droplets for Ab production and accumulation within the droplet; generation of large numbers of virus-encapsulated water-in-oil emulsion droplets; one-to-one merging of the two droplet populations for the produced Abs to bind to viruses; generation of large numbers of host-cell-encapsulated water-in-oil emulsion droplets; merging of these host-cell-encapsulated droplets

with the previously merged Ab-producing cell/virus-encapsulated droplets; co-cultivation, during which time infection and/or neutralization of host cells occur; flow-through optical identification of infection and/or neutralization to identify cells that produce nAbs (Fig. 1A, sequentially from left to right panels). Fig. 1B shows images of the microfabricated system and device micrographs demonstrating the various functional droplet steps; droplet generation, droplet merging, droplet culture/optical identification.

Importantly, the microfluidic system that integrates all of these steps is capable of fully automated operation through a LabView-controlled computer interface, allowing for the continuous operation of the PRESCIENT platform with minimal human intervention. This minimization of manual sample handling, which improves biological safety and reduces the possibility for human error, enhances the overall platform stability. Each of the functional components of the PRESCIENT device, namely cell-encapsulated droplet generation, incubation of droplets, merging of droplets, detection of droplet contents using an optical setup (currently based on microscopic imaging, and to be changed to flow-through fluorescence detection in the future), follow well-established techniques and instrumentation configurations widely utilized in the field of droplet microfluidics (27-31).

We analyzed and characterized each aspect of the PRESCIENT platform verifying platform stability and performance. First, we demonstrated that the system produced uniform cell-encapsulated 150 μm diameter droplets containing either host cells, viral particles, or Ab-secreting hybridoma cells using a T-junction droplet generator (Fig. 1B; Steps 1, 4a, 8a). Then, we demonstrated, characterized, and optimized one-to-one droplet merging using 3D electrodes (Fig. 1B; Steps 4b & 8b), followed by on-chip incubation (Fig. 1B; Steps 2 & 6) and optimization of culture conditions. Finally, we showed that droplets containing fluorescently labeled cells can be correctly identified (Fig 1B; Step 10). The overall assay speed (considering a single droplet going through the entire sets of steps) was in the range of 3 – 10 droplets/sec. Prototype devices used in this study were fabricated using the standard PDMS soft lithography approach.

Viral Infection and Neutralization Model

The following viral infection and neutralization model was utilized for both the multi-well plate and in-droplet experiments: (1) a replication-competent GFP-tagged murine hepatitis virus (MHV-A59 EGFP) that infects L2 host cells and expresses GFP upon replication (32); (2) L2 host cells that are susceptible to MHV-A59 EGFP infection (33), (3) an anti-MHV-A59 nAb-producing hybridoma

line A2.1 (34), and (4) a non-neutralizing irrelevant Ab-producing hybridoma line J558L that served as negative control (35). MHV-A59 EGFP was selected as an attractive viral system for these studies as it is a well-studied model system that is readily available, thoroughly characterized, and is non-pathogenic to humans, thus providing low risk associated with its usage (36) during platform development and characterization. In this system, GFP-positive expression in host cells indicate host cell infection, and the lack of GFP expression indicates neutralization of MHV-A59 EGFP infection of host cells.

Multi-well Plate Infection and Neutralization Assay

Multi-well plate assays were initially conducted to identify an approximate cell viability range and host cell infection efficiency. First, two different base media, DMEM and RPMI 1640, were tested to determine which one supports optimal infection efficiency. In RPMI, infection of L2 cells was first observed at approximately 5 hrs post inoculation (multiplicity of Infection (MOI) = 1) with the fraction of infected cells peaking at 15 hrs, when 65% of the host cells exhibited green fluorescence from the MHV-A59 EGFP infection (Supplementary FIG S2A; red line). In DMEM, infection was again first observed at approximately 5 hrs post-inoculation (MOI = 1), with the percentage of infected cells peaking at 15 hrs with 54% of host cells showing green fluorescence (Supplementary FIG S2A; blue line). Regardless of the media used, cell viabilities were >98% at 48 hrs post seeding (Supplementary FIG S3). RPMI was selected as the base media in all subsequent experiments on the basis of its ability to support efficient replication of MHV in L2 cells, its equivalence to DMEM in supporting the survival of L2 cells, and the superior growth of hybridomas in this medium.

Next, neutralization of host cell infection by Abs produced by A2.1 hybridoma cells known to produce nAbs against MHV-A59 was tested in multi-well plates. In wells infected with virus incubated with supernatants from hybridoma J558L, which produces non-neutralizing Abs, the number of infected host cells (EGFP+) continued to increase, starting from 7 hrs post-inoculation with 6.5% of the host cells infected until peaking at approximately 19 hrs with 60% of the host cells being infected (Supplementary Fig. S4 A & B). In contrast, when supernatants from hybridoma A2.1 that produces nAbs against MHV-A59 were used, infection of 5.5% of the cells was first observed at 13 hrs post-inoculation and then peaked at 19 hrs with 22% of host cells showing evidence of infection (Supplementary Fig. S4 A&C). There was a 3 standard deviation difference in the number of infected cells between the two datasets. This multi-well plate assay

showed that a 7 – 15 hr time point was ideal for determining whether infection has been neutralized by nAbs produced by hybridoma cells, and formed the basis for in-droplet infection and neutralization assay conditions.

In-Droplet Cell Viability

To check the cell viability of L2 host cells and Ab-producing hybridoma cell lines (nAb-producing A2.1 cells and non-nAb-producing J558L negative control cells) in droplets, cells were encapsulated in droplets that contained propidium iodide, a compound that selectively fluorescently stains dead cells. Approximately 5-8 cells were encapsulated per droplet and viability was monitored for 48 hrs, the maximum expected duration of the entire in-droplet assay. At 24 and 48 hrs, the nAb-producing A2.1 cells showed viabilities of 59% and 56% at 24 hr and 48 hr time points (Fig 2A) respectively. At 24 and 48 hrs, the L2 host cells maintained greater than 95% and 93% viability, respectively (Fig 2B). At 24 and 48 hrs, the non-nAb producing J558L cells showed 74% and 68% viability after 24 and 48 hrs, respectively (Fig S5). Lower in-droplet cell viabilities compared to those seen in multi-well plate were likely due to adhesion-induced signaling within the cells that increased their survival (37) as well enhanced nutrient availability when culturing the cells in well plates.

In-Droplet Infection Assay

For the in-droplet infection assay, virus and host cells were first tested at MOIs = 1 & 5. Both MOIs demonstrated similar levels of infection kinetics (data not shown) and, as a result, subsequent experiments were conducted at MOI 1 to allow detection of lower amounts of neutralizing antibody in a droplet. For these in-droplet infection assays, virus and host cells were co-incubated at MOI 1 and infection was assessed. Within approximately 8 hrs, 100% of droplets showed fluorescence (Fig. 2C, orange line with square markers and gray line with circular markers). However, this percentage showed dependence on the number of host cells encapsulated in each droplet (Fig 2C). When using 1-5 host cells per droplet, ~82% of the droplets showed fluorescence, but never reached 100% (Fig 2C, blue line with triangular markers). This percentage, however, increased to 100% after 8 hrs of virus and host cell co-incubation when 6-10 host cells were encapsulated. When using 10-15 host cells in a droplet, again 100% of droplets showed fluorescence, with no difference in the time point at which 100% of droplets showed

fluorescence compared to when 6 – 10 host cells were utilized. Supplementary Figure S6 shows the degree of infection, indicated by green fluorescence, in the host cells encapsulated in droplets. Having 100% of droplets showing fluorescence is needed to have no (or minimum) false-positives, as the assay measures reduction or absence of fluorescence in the host cell-containing droplets if nAbs neutralize the infection. Thus, the target concentration of host cells in droplets was set to 6-8 cells per droplet for all subsequent in-droplet assays. When applying the developed droplet microfluidic system to different viral infection system, the number of host cells per droplet most likely have to be re-characterized and optimized, as the depending on the viruses, the degree of infection of host cells can vary vastly.

In-Droplet Neutralization Assay

To test whether nAb-producing hybridoma cells encapsulated in droplets can prevent host cells from being infected, an in-droplet neutralization assay was conducted at a multiplicity of infection (MOI) of 1 in the presence of nAb-producing (A2.1) and a non-nAb-producing (J558L) hybridoma cells following the full multi-step droplet assay illustrated in Fig. 3. As seen in Fig. 3A & B, when a single J558L cell was encapsulated in a droplet, there was robust infection of host cells (Fig. 4A; bottom two rows, 'GFP' column) compared to those that had a single A2.1 cell encapsulated in a droplet (Fig. 4B; bottom two rows, 'GFP' column). Monitoring the degree of infection in these two different cell populations over time showed that infection was significantly neutralized. This result clearly demonstrate that a single nAb-producing hybridoma cell can neutralize the infection of host cells by MHV within a droplet format. Mean fluorescent intensity analysis was conducted at 12 hrs and 18 hrs (Fig. 4C) based on the time-series in-droplet infection percentages shown in Fig. S8. Compared with J558L cells, the nAb-producing A2.1 cells exhibited a neutralizing capability difference of greater than 3 standard deviations from 9 to 15 hrs after the droplet containing hybridoma cells and viral particles was merged with the host cell-containing droplet and co-incubated (Fig. S8). However, by ~18 hrs, even droplets that contained nAb-producing A2.1 cells showed host cell infection percentages somewhat similar to those that contained non-nAb-producing J558L cells. However, those nAb-containing droplets displayed noticeably lower fluorescent intensities (i.e., infection) when compared to the non-nAb-containing droplets at both the 12 hr and 18 hr timepoints. This result shows that for nAb-producing hybridoma cells to be successfully identified, neutralization measurement should be conducted between 8 to 16 hrs, with 12 hrs post-merging/incubation being the optimum time point to see maximum differences in the degree of host cell infection.

Discussion

In this work we have demonstrated the capability of utilizing droplet microfluidics bioreactors to efficiently differentiate and identify neutralizing Ab-producing cells from non-neutralizing Ab-producing cells through a direct functional assay. Viral infection of host cells was successfully demonstrated, followed by demonstration that a single nAb-producing hybridoma cell encapsulated in a droplet is sufficient to neutralize viral infection of host cells in droplet format. These two results, demonstrated for the first time in droplet format, opens up many possibilities in translating various viral infection and neutralization assays into high-throughput droplet microfluidics format. Although in this first prototype fluorescence imaging-based method was utilized to identify neutralization events, the fluorescent intensity analysis results show that a fluorescent intensity threshold could be set for a laser-based photomultiplier tube detection of droplet fluorescence in a flow-through format. This opens up the possibility to conduct flow-through detection and sorting of droplets to isolate droplets showing no infection (“hits”; GFP-) to a collection chamber for further downstream analysis and processing, while sending droplets that showing infection (waste; GFP+) into a waste channel. In summary, this work establishes the PRESCIENT concept as a potential engine for discovering nAbs of significant therapeutic interest against viral pathogens.

The PRESCIENT system offers several advantages over conventional approaches. First, we have devised and demonstrated a method to identify nAb-producing cells at single cell resolution by directly measuring whether the produced Ab can actually prevent the infection of host cells by the virus. At this time, this marks the first droplet microfluidic device capable of distinguishing the neutralizing capability of Abs produced from a single cell. Second, droplet microfluidic systems have been developed and used extensively in the past decade with a wide variety of biological and synthetic organisms to enable extremely high-throughput assays. By creating a direct functional neutralization assay into such droplet format, the development here opens up the possibility of conducting high-thoughput screening using this powerful assay. Third, the ability to rapidly analyze and detect nAb-secreting cells should also allow the identification of Ab-dependent infection enhancement, which can potentially provide exceptional insight into the function of specific Ab-producing cells at a throughput that could have been of high interest during several global pandemics, such as the 2003 severe acute respiratory syndrome (SARS) epidemic, the 2009 influenza H1N1 pandemic, the 2015 Middle East respiratory syndrome coronavirus (MERS-CoV) outbreak, the more recent Ebola and Dengue virus outbreaks, and the

currently on-going 2019 novel coronavirus outbreak (2019-nCoV). Finally, it should be noted that the developed PRESCIENT strategy has the potential to dramatically accelerate the analysis of immune responses to viral infection, harvesting nAb-producing cells, and developing vaccines that elicit protective nAbs. This work also lays the foundation for using the PRESCIENT platform as a vital tool for identifying Abs that neutralize viral pathogens while performing functional neutralization assays at single-cell resolution with unprecedented speed.

Despite these advantages and potential, the current prototype PRESCIENT system has several limitations in its current form, both from technological perspective as well as from biological perspective. First, the multiple steps required to test the neutralization capability of Abs produced by cells require multiple droplet operation steps, such as multiple droplet merging steps and multiple droplet incubation steps. Although droplet microfluidics is a powerful high-throughput sample handling technology and many droplet manipulation technologies are well characterized, integrating many functions in a sequential manner to perform a complex multi-step assay while handling very large number of samples remain a formidable challenge. In sequential assays, any error or low efficiency in a particular assay steps can add up and lead to overall low system efficiency and/or high error rate. Thus, the current PRESCIENT system still requires further characterization and integration of each of the multiple droplet manipulation steps, as well as further development into how to best integrate these steps with high efficiency and low error, as we have demonstrated for various other droplet microfluidics applications (27, 28, 31, 38).

Second, there are inherent biological limitations that present challenges to the PRESCIENT system. For most viral systems, such as MHV used here, not all host cells are infected by viruses even at high titer. For example in the case of MHV used here, to achieve initial infection of >99% of the cells to provide maximal fluorescent signal, it was necessary to use an MOI of 5, where the higher the MOI used is, the more difficult it could become to detect nAbs. Hence, while a high MOI is needed to infect most host cells (which is highly virus-dependent), such high MOI poses a challenge in neutralizing large numbers of viral particles using Abs produced by only one or a small number of Ab-producing cells. Thus, multi-timepoint screening steps, along with other recent advances in droplet microfluidics such as our first-in first-out approach (39), may have to be utilized to overcome these challenges. In addition, the proposed approach requires the use of viral reporter systems. Fortunately, reporter system for many viral pathogens of global consequence, including Human Immunodefieciency Virus (HIV) and influenza have been developed (40-44), thereby setting the stage for future studies using the PRESCIENT system.

Despite these limitations, the presented platform still provide a powerful and broadly applicable toolset. The broader impact of such a screening platform extends beyond the realm of Ab identification and epitope design, but also has the potential to transform the way in which we conduct assays to develop new therapeutics and vaccines against broad ranges of viruses and biothreat agents.

Author Contributions

J.A.W., H.W., J.L, P.dF., and A.H. designed research; J.A.W., H.W., J.T., J.L, P.dF., and A.H. performed research; J.T., J.L, P.dF., and A.H. contributed new reagents/analytical tools; J.A.W. and H.W. analyzed data; J.A.W, J.L, P.dF., and A.H. wrote the paper.

Acknowledgements

This project was initially supported in part by funding from the Texas A&M Clinical Science & Translational Research Institute Pilot Grant #CSTR2016-1 to A. Han/P. de Figueiredo/J. Leiboiwitz and by the Department of Defense Graduate SMART Scholarship to J. Wippold. The later stage of the project was supported by the National Institutes of Health (NIH) / National Institute of Allergy and Infectious Diseases grant 1R01AI141607-01A1. We would like to gratefully acknowledge Dr. Susan Weiss of the University of Pennsylvania for providing the MHV-A59-EGFP virus, Dr. Wendy Gilmore of the University of Southern California for providing us with the A2.1 hybridoma, and Dr. Koichi Kobayashi of Texas A&M University for providing us with the J558L hybridoma.

Conflicts of Interest

Authors of this work have applied for patent protection of the developed technology.

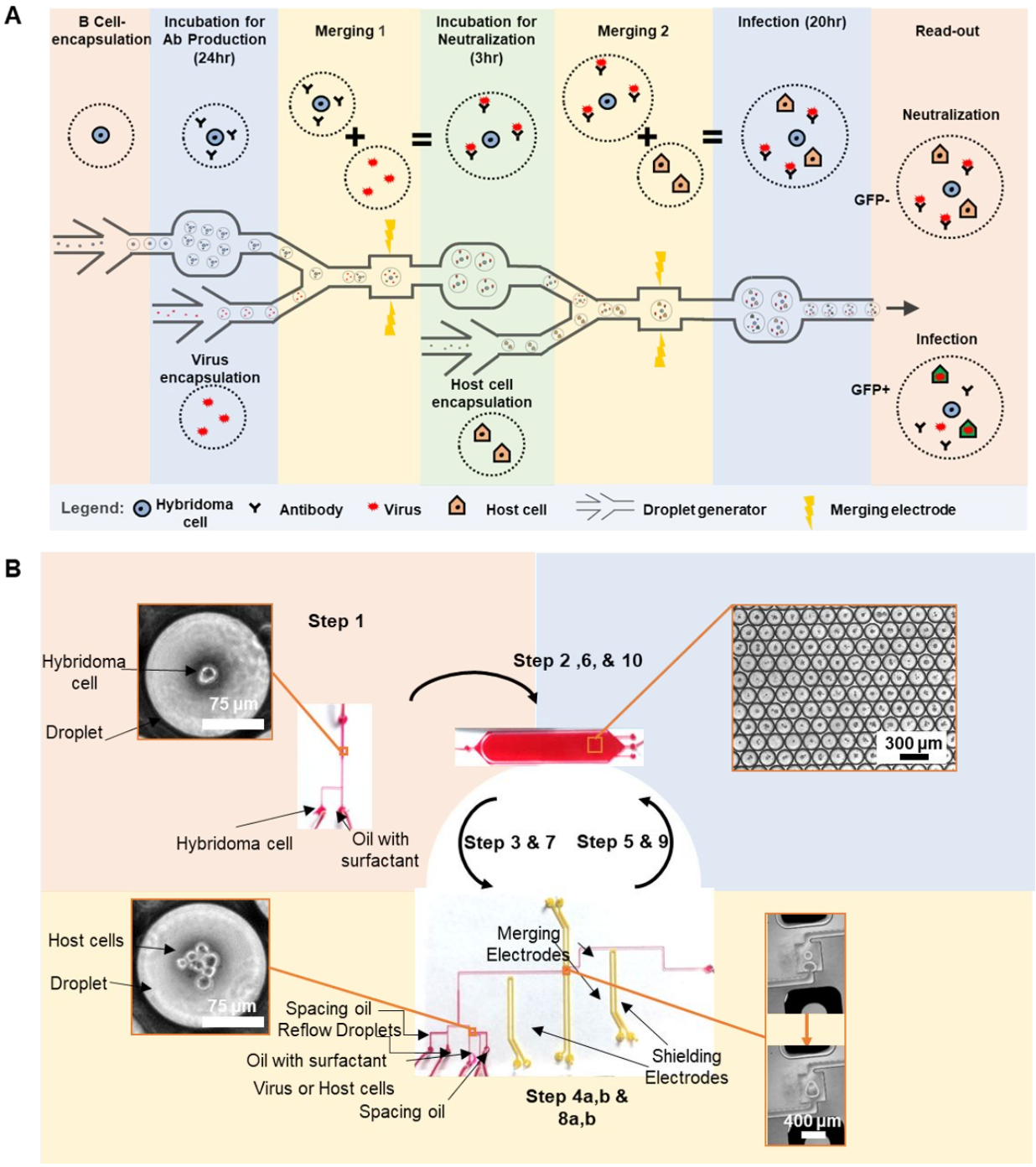

Figure 1. (A) Two-dimensional schematic of the PRESCIENT workflow. (B) The developed PRESCIENT prototype device that is composed of three chips that are interconnected through tubing. Detailed protocol steps from (A) are labeled in (B) as follows: 1) Droplet generator to encapsulate Ab-producing cells into droplets; 2) Incubation chamber to allow for in-droplet Ab production; 3) Reflow droplets into

merging device. 4a) Droplet generator to encapsulate MHV particles into droplets; 4b) Droplet merging region to merge virus-rich droplets with Ab-rich droplets; 5) Flow merged droplets into incubation chamber; 6) Incubation chamber to allow for Ab interaction with viral particles in droplet; 7) Flow droplets into merging device; 8a) Droplet generator to encapsulate host cells into droplets; 8b) Droplet merging region to merge viral/Ab-rich droplets with host cell droplets; 9) Optical detection region to visualize infection or neutralization. Red = Fluidic Channels; Yellow = Merging (center) & Shielding (left and right) Electrodes. (B) Microscopic images of key parts of each microfluidic chips that compose the integrated PRESCIENT microfluidic system. Each color panel indicate each microfluidic chip.

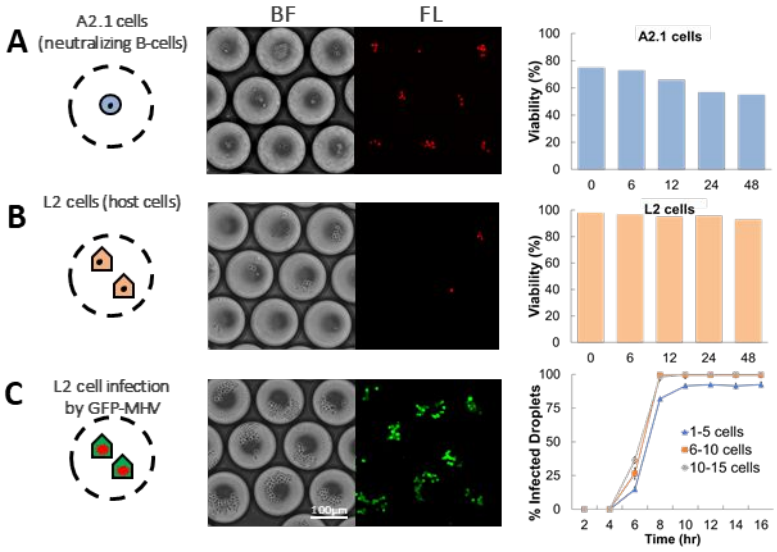

Figure 2. Results from on-chip verification of individual protocol steps. (A) displays a bright-field image on the left with its corresponding fluorescent image on the right showing dead A2.1 hybridoma cells. Viability data is presented in the bar graph to the right of the fluorescent droplet image. SEM < 1% for all timepoints. (B) displays a bright-field image on the left with its corresponding fluorescent image on the right showing dead L2 host cells. Viability data is presented in the bar graph to the right of the fluorescent droplet image. SEM < 2% for all timepoints. (C) displays a bright-field image on the left with its corresponding fluorescent image on the right showing infected L2 host cells. SEM < 4% for all timepoints. Droplet infection data is presented in the line graph to the right of the fluorescent droplet image.

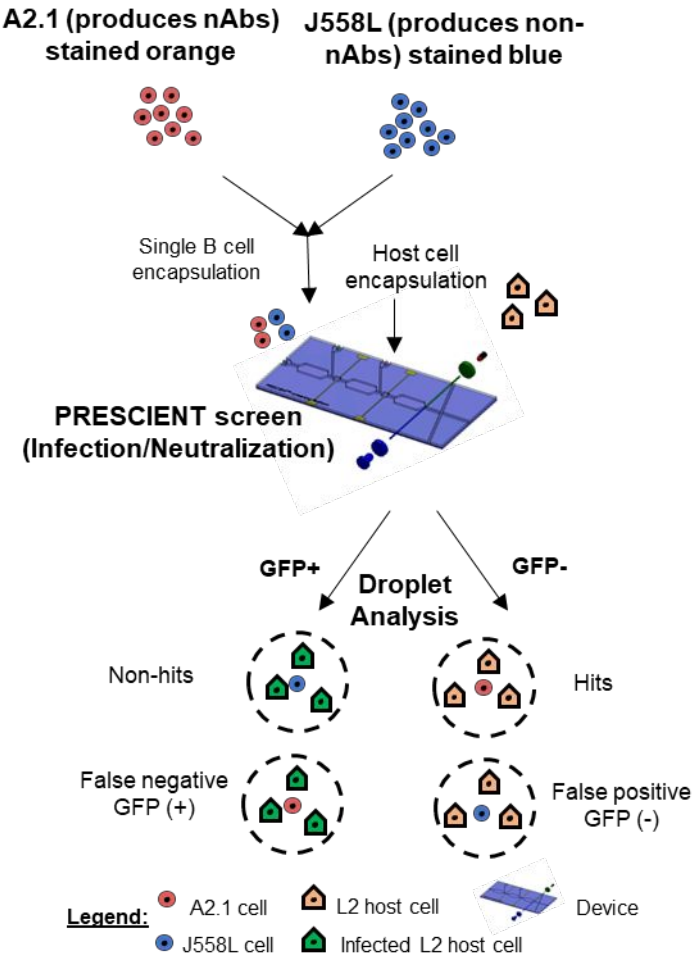

Figure 3. 2D schematic of single antibody producing cell neutralization assays using stained hybridoma cell populations.

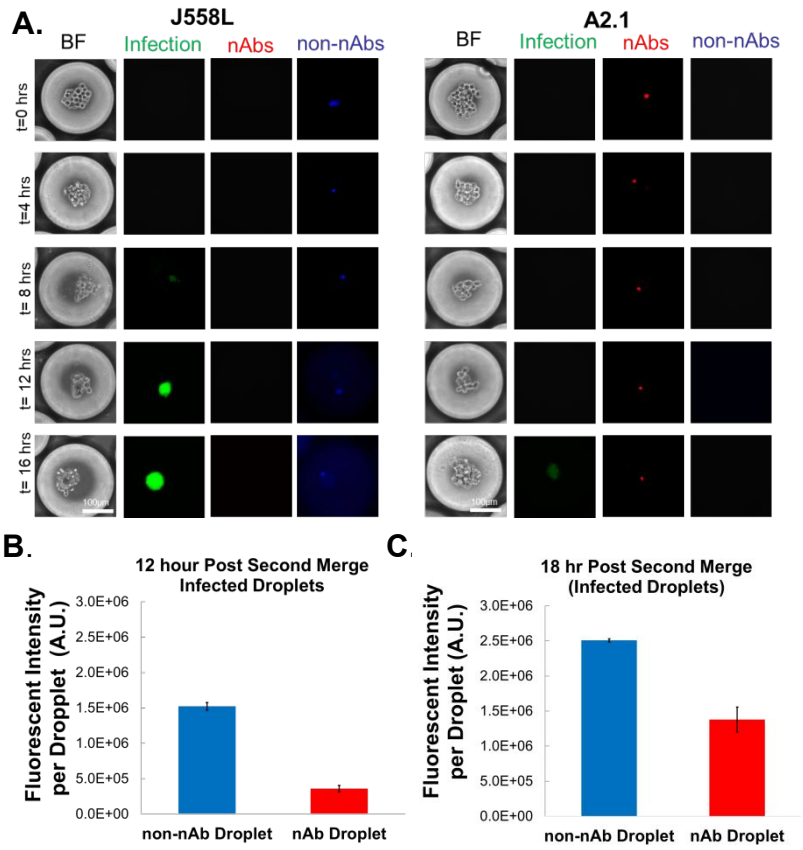

Figure 4. (A) Experimental micrographs demonstrating infection in the presence of a single non-nAb producing cell (J558L column) and neutralization in the presence of a single nAb (A2.1 column) producing cell. (B&C) Graphs comparing mean fluorescence intensity from analyzed infected droplets obtained from single hybridoma cell PRESCIENT assay from the 12 hr (B) and 18 hr (C) post-final droplet merge timepoints. (Errors are denote standard deviation between three identical experiments).

Methods

Device Fabrication

In this work, we establish the first working prototypes for devices that are proficient in evaluating antibody producing cells for functional analysis. PRESCIENT is fabricated using standard PDMS based soft lithography techniques (45). The droplet microfluidic devices used for performing aforementioned experiments consists of three functional components on separate but tethered chips; droplet generation, droplet merging, and droplet incubation (Fig. S1). Initial hybridoma cell droplet generation (diameter 150 μm) is accomplished using a single T-junction droplet generator comprised of a horizontal carrier oil channel (150 μm wide) and a perpendicular water channel (120 μm wide), both with a height of 100 μm. A droplet culture and observation device is used to enrich Abs produced by hybridoma cells encapsulated in their respective droplets, allowing co-cultivation of Ab rich droplets and viral particles, serving as an infection/neutralization chamber. The device exploits 400 μm x 400 μm pillars spaced 50 μm apart, serving as an in-house designed massive basket-like trapping chamber for a monolayer of droplets to be collected, analyzed, and observed within a microfluidic chamber (10 mm x 3 mm). The height of the culture chamber was set to 353 μm to allow for single droplet layer observation of triple merged 150 μm droplets (resultant = 210 μm) while ensuring minimal pressure buildup. The droplet merging device consists of five inlets; the first inlet is used to reinject droplets from the culture device into the merging device using a syringe-based flow driven pump (Chemyx Fusion 200 model, TX) and medical grade tubing (Tygon ND-100-80 01.X.03X500 (VWR #89404-300) for transferring droplets between tethered devices. The two carrier oil outer inlets (See annotation in Fig. S1) evenly space droplets during reinjection of the incubated droplets and production of the newly generated droplet population. The inner two inlets are used to introduce cells and fluorinated oil (Novec 7500, 3M) with surfactant (2.5 wt/wt %, Pico-Surf 1™, Dolomite Microfluidics, MA) generating a new train of droplets. The two trains of droplets flow parallel to one another and undergo passive synchronization by way of a harmonization channels that use a series of 100 μm x 100 μm pillars with 100 μm gaps that allow for the synchronization of opposing droplet pairs exiting the harmonization channel, producing a 1:1 ratio of droplet pairing necessary for high efficiency downstream droplet merging. The droplet pairs enter a 100 μm wide and 100 μm high channel using a Y-shaped junction. The merging region was 400 μm wide and 450 μm long, which prepares droplets for merging by reducing the droplet speed and allowing paired droplets to make physical contact with one another. The merging channel has a 75 μm inlet and a 100 μm wide outlet to accelerate the droplets prior to entering and exiting the designated merging channel,

which in turn increases the collision-relaxation force, in combination with the E-field this increases the induced droplet electrocoalescence efficiency. As 3D electrodes have proved to be more efficient in merging droplets using lower input voltages, more uniform E-fields, and therefore lower locally induced electric fields, we employ 3D electrodes in order to provide this platform with a distinct advantage over other microfluidic technologies. The 3D electrodes are introduced using a specialized metal (Roto144F Low Melt Fusible Allot – Field's Metal, RotoMetals, CA) that is liquid at high temperatures and solid at room temperature and is introduced into predesignated microchannels that were fabricated during the microfluidic channel fabrication process (Fig S1, yellow). The liquid metal is drawn into the microcavity using low temperature heat resistant FEP tubing (IDEX Health & Science LLC, #1520L, WA) to apply a suction force using a syringe. The entire merging device microchannel height was set to 120 μm.

For obtaining 353 μm thick microchannel patterns, a master silicon wafer was spin-coated with negative photoresist (SU-8 2075, Microchem Corp., MA) at 1500 rpm, followed by soft-baking in two steps at 65℃ and 95℃ for 24 hr and 20 min, respectively. After this initial photoresist coat and bake, the same procedure was carried out one additional time as a double-spincoat in order achieve the desired thickness. Following the soft-bake, the master was exposed to ultraviolet (UV) light using a standard photolithography mask aligner (MA6 Karl Suss, Suss MicroTec, Germany) and post-exposure baked at 65℃ and 95℃ for 40 min and 20 min, respectively. After developing the unexposed photoresist (EBR 10A, Microchem Corp., #10018079, MA), the patterned wafer was (tridecafluoro-1,1,2,2 tetrahydrooctyl) trichlorosilane (United Chemical Technologies, Inc., Bristol, PA) coated for 20 min using a conventional desiccator, to preventing pattern removal during PDMS replication. For obtaining 120 μm thick microchannel patterns, a master silicon wafer was spin-coated with negative photoresist (SU-8 2075, Microchem Corp., MA) at 1750 rpm, followed by soft-baking in two steps at 65℃ and 95℃ for 24 hr and 20 min, respectively. Following the soft-bake, the same master mold preparation procedure was carried out as described for the completion of the 350 μm height master mold. A thin poly(dimethylsiloxane) (PDMS, Sylgard® 184, Dow Corning Corp., MI) layer (thickness: 30 μm) was spin-coated on the patterned glass slide at 3000 rpm for 30s to obtain a hydrophobic bottom surface that is necessary for droplet generation. For all three functional devices, a PDMS microchannel was replicated from the master by pouring 20g of PDMS mixture (1:10 curing agent to polymer) onto the master secured in a plastic petri-dish. After polymerization, the merging device is bonded to the PDMS-coated glass slide using conventional oxygen plasma treatment (Plasma cleaner, Harrick Plasma, Ithaca, NY) for 90s. After polymerization, the droplet generator and culture chamber microchannels were

bonded to a PDMS-coated glass slide (Micro Slides 2947- 75x50, Corning Inc., NY) using the same oxygen plasma treatment protocol. All PDMS microchannels were filled with a commercial hydrophobic surface coating agent (Aquapel, PPG Industries) and flushed with the same fluorinated oil prior to use. The fabrication of the working PRESCIENT prototypes marks an important milestone in the development of a fully automated, high-throughput antibody producing cell screening platform.

Multi-well plate confirmatory assays

Prior to platform characterization of our microfluidic droplet-based system, we characterized various biological conditions and assay relevant factors using a bulk multi-well plate approach, enabling a smooth and efficient transition to the comparable droplet confirmation assays. We investigated differences in infection rate and cell proliferation induced by different cell culture media, (MOI), and required incubation times for adequate antibody production. MOI gives you the anticipate ratio between viral particles to host cells. We characterized two commonly used and well-known cell medias (Dulbecco's Modified Eagle Media & Roswell Park's Medical Institute 1640) often used for infection experiments, providing optimal cellular conditions conducive to wide spread MHV-A59 EGFP infection (see Fig S2). We characterized cell growth of the A2.1 hybridoma cell line using a glutamine supplement (GlutaMAX ™ Supplement, Thermo Fisher # 35050061), which is known to enhance cell viability when compared to non-supplemented base medias. In triplicate, cells were seeded at 1x10^5 cells/mL in wells of a multi-well plate using culture media and monitored for cell viability at 0, 3, 6, and 9 hr using 10 µg/mL of a fluorescent dead cell stain (Propidium Iodide, Thermo Fisher # P3566). Viability was calculated as $\left(\frac{number\ of\ total\ cells - number\ of\ fluorescent\ cells}{number\ of\ total\ cells}\right) \times 100$. For determining the optimal base media for infection, 2x10^5 host cells were seeded in wells of a multi-well plate and incubated with either DMEM or RPMI 1640 media for 2 hrs before adding virus (MOI 1) to the wells. Infection was monitored over 17 hrs using the GFP reporter encoded into the MHV genome. Infection was calculated as $100 - [\left(\frac{number\ of\ total\ cells - number\ of\ fluorescent\ cells}{number\ of\ total\ cells}\right) \times 100]$. For determining optimal antibody production time, we conducted a multi-well plate neutralization assay in which antibody producing cells were seeded at a concentration of 1x10^6 cells/mL and cultured for 24 and 48 hrs to allow accumulation of secreted antibodies. Supernatant from the wells were harvested and mixed at a 1 to 1 ration with virus (8 µL containing 2x10^5 PFU) and incubated for 3 hrs at 37 C and 5% CO_2. The supernatant and virus mixture was then aliquoted into wells of a 24-well multi-well plate containing 2x10^5 host cells in 500 µL media. Infection was calculated using the same

formula as in the aforementioned multi-well plate infection assay. These multi-well plate characterization assays shed crucial insight as to the validity of the proposed biological strategy employed in the droplet microfluidic screening system.

Droplet Cell Viability

The cellular components of our system were analyzed for microdroplet cell viability using a two-step approach. First, MHV-A59 EGFP neutralizing hybridoma cell viability was demonstrated and characterized in a droplet culture. For this experiment, we concentrated $6x10^6$ A2.1 cells in 500µL RPMI media in conjunction with propidium iodide (PI) dead cell stain at 10µg/mL for long-term cell viability analysis. Propidium Iodide dissolved in ultrapure water and maintains stability over 14 days (46). The suspension was then used to generate droplets of 150 µm in diameter. The droplets flowed from the droplet generator device into the culture device and were monitored over 48 hrs using fluorescent microscopy to distinguish between live and dead cells. Second, MHV-A59 EGFP susceptible host cell viability was determined in a droplet culture. For this experiment, we concentrated $6x10^6$ L2 cells in 500 µL of RPMI media along with a propidium iodide dead cell stain at 10 µg/mL. The suspension was then used to generate droplets of 150 µm in diameter. Similar analysis was conducted over 48 hrs using fluorescence microscopy to identify the dead cells. Through these assays, we demonstrate PRESCIENT's capability of maintaining cellular functionality and assume this capability extends beyond the cell lines presented here but with a wide variety of contrasting and distinctive cellular species.

Droplet Infection

As an integral facet of the PRESCIENT workflow, we demonstrate not only the ability to infect cells in a highly controlled and semi-automated environment, but also the ability to monitor the progression of infection in real-time. Rates of MHV-A59 EGFP infection of L2 host cells were determined in a droplet culture experiment. For this experiment, we concentrated $6x10^6$ L2 cells in 150µL RPMI media and added MHV-A59 EGFP to the cell suspension at a MOI of 1. The suspension was then used to generate droplets with 150 µm in diameter using the droplet generator. The droplets are introduced to the culture chamber device and monitored over 36 hrs using fluorescence microscopy to identify infected cells. We comprehensively analyzed not only the overall percentage of fluorescent droplets but also the overall percentage of fluorescent cells. Furthermore, we performed an in-droplet comparison of samples at a MOI of 1 and MOI of 5 to determine which MOI is capable of achieving robust infection while using the fewest number of

viral particles. The validation of in droplet, real-time infection monitoring proves to be one of PRESCIENT's key features at the crux of this platform's success.

Droplet Neutralization

The ability to monitor infection, and the lack thereof, at a high resolution is at the core of PRESCIENT. The demonstration of single cell neutralization marks a major milestone in vaccine discovery, but also for successive vaccine development and immunotherapeutic design. The in droplet MHV-A59 EGFP neutralization capability was demonstrated by concentrating $1.5x10^6$ neutralizing A2.1 hybridoma cells in 500 µL of RPMI media and generating 150 µm droplets, followed by subsequent incubation in the culture chamber device for 24 hrs. After a 24 hr incubation to accumulate nAbs in their respective droplets, the droplets are flowed from the culture chamber into the merging device in such a way that simultaneously generated and synchronized droplets containing MHV-A59 EGFP were paired one-to-one with nAb rich droplets. The droplet pairs were merged using electrocoalescence by inducing an electric field that is generated by introducing a 3V 25kHz sinusoidal wave from a waveform generator (Agilent, #33120A, CA) to a high voltage amplifier (Trek Inc, Model 2210, NY), amplifying the signal by approximately 100X before sending the signal to the merging device. Merged droplets are then cultured in a culture chamber for 3 hrs to allow for neutralization of the virus to occur. Last, these droplets are flowed from the culture chamber and again similarly merged in such a way that simultaneously generated droplets of L2 host cells are paired one-to-one with the preexisting virus/nAB droplets. The resulting droplets are then reintroduced into the culture chamber and incubated for 36 hrs allowing for monitoring of viral neutralization using fluorescence microscopy.

Testing the functionality and resolution of the PRESCIENT system we utilize biocompatible cell-staining dyes preloaded with $1.5x10^6$ hybridoma cells and washed to enable facile visualization of specific cell populations during the experimental assays, as shown in Fig. 4. First, two homogeneous dye-labeled populations of hybridoma cells are prepared. The first cell line, cloned neutralizing A2.1 human hybridoma cells, are stained with an orange-colored dye (i.e., labeled with CellTracker Orange CMRA). The second cell line, non MHV-A59 EGFP neutralizing Ab producing J558L hybridoma cells, are stained with a blue colored dye (i.e., labeled with CellTracker Blue CMF_2HC). We separately encapsulate these two populations of labeled cells in droplets, and through a series of droplet merging events similar to those described in the previous section, we identify droplets that permit MHV-A59 EGFP infection. Droplets which are defined as

having a GFP fluorescent signal three standard deviations (SD) greater than droplets containing uninfected host cells serving as an internal control. Finally, we track the rate at which the system accurately identifies neutralization (GFP^-, red^+) and non-neutralization (GFP^+, $blue^+$) of Ab-producing hybridoma cells. We chose to combine GFP (MHV-A59 EGFP), blue (non-neutralizing), and red (neutralizing) colors due to their distinct excitation and emission spectra, allowing for simultaneous fluorescent analysis. False positives are identified as GFP^-, $blue^+$, red^- droplets. False negatives are identified as GFP^+, $blue^-$, red^+ droplets. The aforementioned fluorescently tagged hybridoma cell experiment enables the facile estimation of the false-positive and false-negative frequencies. By dividing the number of false positives or false negatives over the total number of droplets analyzed, we accurately determine the corresponding frequencies and subsequently the overall platform efficiency. This work lays the foundation for utilizing PRESCIENT as a premier platform for identifying neutralizing Abs and single Ab producing cells that neutralize viral pathogens of possible clinical relevance.

REFERENCES

1. Hey A (2015) History and Practice: Antibodies in Infectious Diseases. *Microbiology spectrum* 3(2):Aid-0026-2014.
2. Chames P, Van Regenmortel M, Weiss E, & Baty D (2009) Therapeutic antibodies: successes, limitations and hopes for the future. *British journal of pharmacology* 157(2):220-233.
3. Strohl W (2014) Antibody Discovery: Sourcing of Monoclonal Antibody Variable Domains. *Current Drug Discovery Technologies* 11.
4. Lim APC, Chan CEZ, Hanson BJ, & MacAry PA (2014) The role of phage display in therapeutic antibody discovery. *International Immunology* 26(12):649-657.
5. Geyer CR, McCafferty J, Dübel S, Bradbury ARM, & Sidhu SS (2012) Recombinant Antibodies and In Vitro Selection Technologies. *Antibody Methods and Protocols*, eds Proetzel G & Ebersbach H (Humana Press, Totowa, NJ), pp 11-32.
6. Traggiai E*, et al.* (2004) An efficient method to make human monoclonal antibodies from memory B cells: potent neutralization of SARS coronavirus. *Nature medicine* 10(8):871-875.
7. Chiu ML & Gilliland GL (2016) Engineering antibody therapeutics. *Current Opinion in Structural Biology* 38:163-173.
8. Smith SA & Crowe JE, Jr. (2015) Use of Human Hybridoma Technology To Isolate Human Monoclonal Antibodies. *Microbiology spectrum* 3(1):Aid-0027-2014.
9. Fanning LJ, Connor AM, & Wu GE (1996) Development of the immunoglobulin repertoire. *Clinical immunology and immunopathology* 79(1):1-14.
10. Ter Meulen J (2011) Monoclonal antibodies in infectious diseases: clinical pipeline in 2011. *Infectious disease clinics of North America* 25(4):789-802.
11. Sparrow E, Friede M, Sheikh M, & Torvaldsen S (2017) Therapeutic antibodies for infectious diseases. *Bulletin of the World Health Organization* 95(3):235-237.

12. Ebersbach H, Proetzel G, & Zhang C (2012) Antigen presentation for the generation of binding molecules. *Methods in molecular biology (Clifton, N.J.)* 901:1-10.
13. Flego M, Ascione A, Cianfriglia M, & Vella S (2013) Clinical development of monoclonal antibody-based drugs in HIV and HCV diseases. *BMC medicine* 11:4-4.
14. Modjtahedi H, Ali S, & Essapen S (2012) Therapeutic application of monoclonal antibodies in cancer: advances and challenges. *British medical bulletin* 104:41-59.
15. H. Shih H (2013) Discovery Process for Antibody-Based Therapeutics. *Development of Antibody-Based Therapeutics: Translational Considerations*:9-32.
16. Baccouche A*, et al.* (2017) Massively parallel and multiparameter titration of biochemical assays with droplet microfluidics. *Nat Protoc* 12(9):1912-1932.
17. Terekhov SS*, et al.* (2017) Microfluidic droplet platform for ultrahigh-throughput single-cell screening of biodiversity. *Proceedings of the National Academy of Sciences* 114(10):2550-2555.
18. Mashaghi S, Abbaspourrad A, Weitz DA, & van Oijen AM (2016) Droplet microfluidics: A tool for biology, chemistry and nanotechnology. *TrAC Trends in Analytical Chemistry* 82:118-125.
19. Ge X*, et al.* (2016) Microfluidic technology for multiphase emulsions morphology adjustment and functional materials preparation. *Chinese Journal of Chemical Engineering* 24(6):677-692.
20. Shembekar N, Chaipan C, Utharala R, & Merten CA (2016) Droplet-based microfluidics in drug discovery, transcriptomics and high-throughput molecular genetics. *Lab Chip* 16(8):1314-1331.
21. Shang L, Cheng Y, & Zhao Y (2017) Emerging Droplet Microfluidics. *Chemical Reviews* 117(12):7964-8040.
22. Liu Z-M, Yang Y, Du Y, & Pang Y (2017) Advances in Droplet-Based Microfluidic Technology and Its Applications. *Chinese Journal of Analytical Chemistry* 45(2):282-296.
23. Xi H-D*, et al.* (2017) Active droplet sorting in microfluidics: a review. *Lab on a Chip* 17(5):751-771.
24. Shembekar N, Hu H, Eustace D, & Merten CA (2018) Single-Cell Droplet Microfluidic Screening for Antibodies Specifically Binding to Target Cells. *Cell reports* 22(8):2206-2215.
25. El Debs B, Utharala R, Balyasnikova IV, Griffiths AD, & Merten CA (2012) Functional single-cell hybridoma screening using droplet-based microfluidics. *Proceedings of the National Academy of Sciences of the United States of America* 109(29):11570-11575.
26. Chaipan C*, et al.* (2017) Single-Virus Droplet Microfluidics for High-Throughput Screening of Neutralizing Epitopes on HIV Particles. *Cell chemical biology* 24(6):751-757.e753.
27. R Guzman A, Kim H, de Figueiredo P, & Han A (2015) *A three-dimensional electrode for highly efficient electrocoalescence-based droplet merging* p 9921.
28. Kim HS, Guzman AR, Thapa HR, Devarenne TP, & Han A (2016) A droplet microfluidics platform for rapid microalgal growth and oil production analysis. *Biotechnology and bioengineering* 113(8):1691-1701.
29. Baret JC*, et al.* (2009) Fluorescence-activated droplet sorting (FADS): efficient microfluidic cell sorting based on enzymatic activity. *Lab Chip* 9(13):1850-1858.
30. Mazutis L*, et al.* (2013) Single-cell analysis and sorting using droplet-based microfluidics. *Nature Protocols* 8:870.
31. Kim HS*, et al.* (2017) High-throughput droplet microfluidics screening platform for selecting fast-growing and high lipid-producing microalgae from a mutant library. *Plant Direct* 1(3):e00011.
32. Das Sarma J, Scheen E, Seo S-h, Koval M, & Weiss SR (2002) Enhanced green fluorescent protein expression may be used to monitor murine coronavirus spread in vitro and in the mouse central nervous system. *Journal of NeuroVirology* 8(5):381-391.
33. Phillips JJ, Chua MM, Lavi E, & Weiss SR (1999) Pathogenesis of chimeric MHV4/MHV-A59 recombinant viruses: the murine coronavirus spike protein is a major determinant of neurovirulence. *Journal of virology* 73(9):7752-7760.

34. Kaufman G, Liu P, & Leibowitz JL (2014) Identification of novel functional regions within the spike glycoprotein of MHV-A59 based on a bioinformatics approach. *Virus research* 189:177-188.
35. Fell HP, Yarnold S, Hellström I, Hellström KE, & Folger KR (1989) Homologous recombination in hybridoma cells: heavy chain chimeric antibody produced by gene targeting. *Proceedings of the National Academy of Sciences of the United States of America* 86(21):8507-8511.
36. Leibowitz J, Kaufman G, & Liu P (2011) Coronaviruses: propagation, quantification, storage, and construction of recombinant mouse hepatitis virus. *Current protocols in microbiology* Chapter 15:Unit 15E.11.
37. Meredith JE & Schwartz MA (1997) Integrins, adhesion and apoptosis. *Trends in Cell Biology* 7(4):146-150.
38. Wang H, Sobahi N, & Han A (2017) Impedance spectroscopy-based cell/particle position detection in microfluidic systems. *Lab on a Chip* 17(7):1264-1269.
39. Dai J, Kim HS, Guzman AR, Shim W-B, & Han A (2016) A large-scale on-chip droplet incubation chamber enables equal microbial culture time. *RSC Advances* 6(25):20516-20519.
40. Nogales A*, et al.* (2019) A Novel Fluorescent and Bioluminescent Bireporter Influenza A Virus To Evaluate Viral Infections. *J Virol* 93(10).
41. Nogales A, Baker SF, & Martínez-Sobrido L (2015) Replication-competent influenza A viruses expressing a red fluorescent protein. *Virology* 476:206-216.
42. Auewarakul P, Paungcharoen V, Louisirirotchanakul S, & Wasi C (2001) Application of HIV-1-green fluorescent protein (GFP) reporter viruses in neutralizing antibody assays. *Asian Pacific journal of allergy and immunology* 19(2):139-144.
43. Montefiori DC (2009) Measuring HIV neutralization in a luciferase reporter gene assay. *Methods in molecular biology (Clifton, N.J.)* 485:395-405.
44. Terahara K*, et al.* (2012) Fluorescent Reporter Signals, EGFP, and DsRed, Encoded in HIV-1 Facilitate the Detection of Productively Infected Cells and Cell-Associated Viral Replication Levels. *Front Microbiol* 2:280-280.
45. Xia Y & Whitesides GM (1998) SOFT LITHOGRAPHY. *Annual Review of Materials Science* 28(1):153-184.
46. Drew J, Donovan M, & Preston H (1993) Stability of propidium iodide stained samples by the coulterR DNA prep workstation for analysis by flow cytometry. *Pathology* 25:17.